IEEE Photonics Journal
An IEEE Photonics Society Publication

Single-Port Superluminescent-Diode Gain-Chip for Tunable Single-Wavelength and Dual-Wavelength Blue-Laser

Volume 13, Number 1, February 2021

Mahmoud N. Eliwa
Abdullah A. Alatawi
Jorge A. Holguín-Lerma
Omar Alkhazragi
Islam Ashry
Tien Khee Ng
Boon S. Ooi

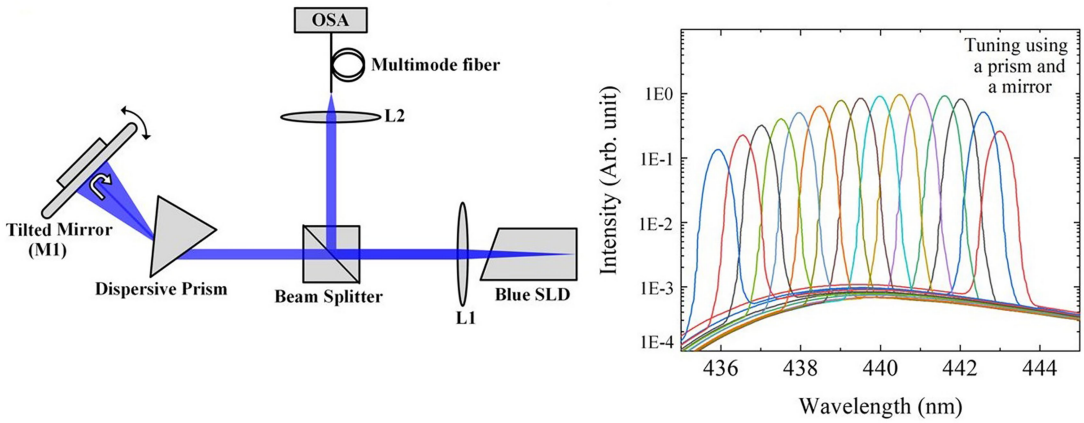

DOI: 10.1109/JPHOT.2020.3046296

Single-Port Superluminescent-Diode Gain-Chip for Tunable Single-Wavelength and Dual-Wavelength Blue-Laser

Mahmoud N. Eliwa, Abdullah A. Alatawi, Jorge A. Holguín-Lerma, Omar Alkhazragi, Islam Ashry, Tien Khee Ng, and Boon S. Ooi

Photonics Laboratory, King Abdullah University of Science and Technology, Thuwal 23955-6900, Saudi Arabia

DOI:10.1109/JPHOT.2020.3046296

Manuscript received November 17, 2020; revised December 12, 2020; accepted December 14, 2020. Date of publication December 21, 2020; date of current version January 4, 2021. This work was supported in part by the King Abdullah University of Science and Technology (KAUST) Office of Sponsored Research (OSR) (OSR-CRG2017-3417) and in part by the KAUST baseline funding BAS/1/1614-01-01 and KAUST CEMSE funding GEN/1/6607-01-01. The work of Tien Khee Ng and Boon S. Ooi was supported in part by King Abdulaziz City for Science and Technology for the establishment of KACST Technology Innovation Center on Solid-State Lighting at KAUST under KACST TIC R2-FP-008. *(Mahmoud N. Eliwa, Abdullah A. Alatawi, and Jorge A. Holguín-Lerma contributed equally to this work.).*
Corresponding author: Boon S. Ooi (e-mail: boon.ooi@kaust.edu.sa).

Abstract: Reconfigurable photonic technology combining multiple functionalities in a single gain-chip is a crucial light-based platform for enabling hybrid applications. Here, we report on achieving a widely tunable and reconfigurable blue laser source using a single-port gain medium based on an InGaN/GaN superluminescent diode (SLD). As compared to tunable laser-diode emitters based solely on stimulated emission from a laser diode used as the gain medium, our amplified spontaneous emission system is capable of fast switching between the stimulated and amplified spontaneous emission regimes for on-demand use of time-incoherent, or time-coherent light with single- or dual-wavelengths. The single- and dual-wavelength laser tunability is designed using various external cavity (EC) configurations for a continuous selection and smooth transition of the emission wavelength from 436 nm to 443 nm. Moreover, the InGaN SLD can amplify the optical power within the EC configuration by 6.5 dB. Thus, the prototype system opens up a viable route for designing reconfigurable light sources based on a single gain chip, and promises disruptive innovation for medical instrumentation, optical sensing technology, and optical communication.

Index Terms: Amplified spontaneous emission, superluminescent diode, tunable laser, InGaN.

1. Introduction

Reconfigurable photonics offering multiple and simultaneous functions are attractive platforms for innovative optical technologies [1], [2]. A crucial aspect of reconfiguring a single photonic system is the ability to smoothly vary the properties of a light source, in order to tailor for different application scenarios. A tunable laser source, for example, finds important applications in Raman and fluorescent spectroscopy, optical sensing, optical communication, and holographic technology [3]–[5]. For visible-light generation, the design of commercially-available tunable laser sources is mainly based on either optical parametric oscillation or fiber-based supercontinuum techniques [6],

[7]. In recent efforts to simplify these systems for niche applications, visible laser diodes used in conjunction with various external cavity (EC) configurations were investigated [8]. By incorporating external optical components to a laser diode, it is possible to control the laser's wavelength and linewidth [8], [9]. Other applications include direct modulation of such tunable laser diodes for dense wavelength-division multiplexing (DWDM) optical communication [10], and future highly dynamic displays [11].

Though EC-laser diodes have attracted significant attention due to their availability, their study is typically complicated, and their operation is relatively unstable [12]. This is because the cavity of the laser diode and the external cavity interact simultaneously to form an effective laser cavity. This is the main cause of drawbacks such as mode hopping and interference based on the feedback optical power provided within each cavity [13]. To address this issue, high-precision anti-reflective (AR) coatings have been developed to suppress the formation of the internal diode cavity and improve the control over the EC-laser [13], [14]. An alternative to AR coatings is the use of a tilted facet or a tilted waveguide such as those found in superluminescent diodes (SLDs), leading to a modal reflectivity below 10^{-5} via a single etching step [15], [16].

Previously, the implementation of tunable lasers based on SLDs in EC configurations focused on the near-infrared and red wavelength regime [17]–[21]. The closest investigations using InGaN-based devices are SLD or its closely-related semiconductor optical amplifier (SOA) inside an EC to generate mode-locked pico-second lasing pulses [22], [23], and narrow-linewidth laser emission for atomic spectroscopy [14]. Nevertheless, combining InGaN-based SLDs with EC configurations has yet to be further explored for tunability and properties achieved herein. Besides, related research on InGaN-based SLDs has continued steadily with particular interests in lighting, displays, and biomedical instrumentation [16], [24]–[26]. These interests have been inspired because the SLD is emitting light in the amplified spontaneous emission (ASE) regime, showing droop-free performance, low temporal coherence, high power density, and low etendue [16], [24], [26]–[30]. These unique optical properties, when implemented in an EC configuration, can offer a reconfigurable single-chip light source capable of emitting both time-incoherent light from the SLD and time-coherent laser light from the EC-SLD, appealing to a wide range of applications, including gas and liquid sensing [31], swept source optical coherence tomography [32], and coherence-convertible light source [33]. As a result, there is a strong motivation to design a stable and reliable visible-light EC-laser using InGaN-based SLDs.

Here, we report on combining a blue-emitting InGaN-based SLD and EC configurations where the SLD gain chip can produce either ASE or tunable laser. We provide continuous control over the laser wavelengths ranging from 436 nm to 443 nm. By using various EC configurations, the SLD-based design provides single- and dual-mode laser tunability. We further prove that the single-port SLD can serve as an amplification medium for the feedback signal provided within the EC. The designed reconfigurable blue-emitting light source would find a myriad of important applications, including free-space and underwater optical communication [34], hybrid coherent-incoherent light-based medical diagnosis [35], and terahertz-wave beat signal generation by dual wavelength photo-mixing [36], and thus advancing the field of reconfigurable laser photonics.

2. Fabrication and Characterization of the InGaN-Based SLD

A blue-emitting InGaN SLD is fabricated on a commercial laser via etching the laser's front facet by 12°, as we described in Refs. [24], [37]. A device length of $\sim$1 mm and a ridge-width of $\sim$15 μm define the injection area of the SLD, having current density as high as 6.7 kA/cm^2 (1000 mA). Depicted in Fig. 1(a), the SLD's gain region exists within an uncoated tilted facet at the output front, and a highly reflective (HR) mirror coating with $>$90% reflectivity on the non-tilted back facet. The 12° angle of the front facet is optimized to avoid reflecting light back into the SLD's internal cavity which consequently prevents the lasing action. The modal reflectivity at different facet angles are found to be below 10^{-5} with tilting angles greater than 6° in GaN-based devices [15], [16], [28]. This characteristic allows us to use the fabricated SLD without the need of adding an AR coating

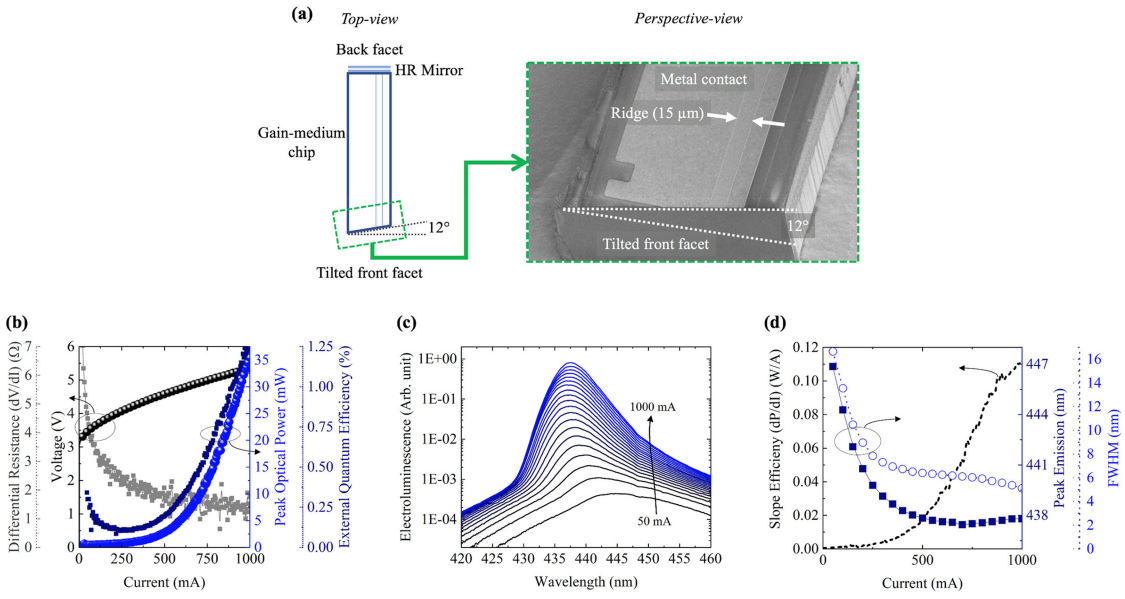

Fig. 1. (a) Top-view schematic (left) and scanning electron microscope image (right) of the InGaN SLD in perspective of the front facet, and showing up the top metal contact, the 15-μm wide ridge waveguide, and the 12° front facet. (b) Light-output–current–voltage (L–I–V), differential resistance (dV/dI), and EQE of the SLD. (c) Optical spectra of the SLD at the different injection current values. (d) Left *y*-axis shows the slope efficiency (dP/dI) as calculated from the L–I curve. Right *y*-axis shows the peak emission and linewidth (FWHM) of the emission spectra.

onto the tilted front facet nor designing a curved waveguide. Comparing with group-III-nitride laser diodes in which it is complicated to obtain dielectric AR with a reflectivity less than 10^{-5}, tilting the SLD's facet offers a simple process to suppress the lasing action [27]. Additionally, the SLD can be fabricated utilizing a commercially available laser diode [37].

The electro-optical characteristics of the designed SLD are shown in Figs. 1(b) and 1(c) when using a pulsed injection current (1-kHz repetition rate, 15% duty-cycle). A pulsed laser diode test system (Keithley, 2520) and an integrating sphere having a silicon photodiode are used to capture the data of Fig. 1(b). The SLD is mounted onto a thermoelectric cooler (TEC, SaNoor, SN-LDM-T) to keep the case temperature of the device at 20 °C. The investigation of the impact of temperature variation on the SLD characteristics has been thoroughly studied in the literature [38] and is out of the scope of this work.

The light-output–current–voltage (L–I–V) characteristics show a turn-on voltage of ∼3.2 V [Fig. 1(b), black circles] and a maximum peak output power of 35.4 mW [Fig. 1(b), blue circles]. The L–I curve of the device is described in terms of linear spontaneous emission from 1 mA to ∼200 mA, followed by the onset of ASE which includes both an exponential increase in the output power from ∼200 mA to ∼800 mA and a gain saturation regime [39] from ∼800 mA to 1000 mA [Fig. 1(b), blue circles]. The differential resistance (dV/dI) shows working values below 2 Ω after the onset of the ASE [Fig. 1(b), gray squares], while the external quantum efficiency (EQE) [Fig. 1(b), blue squares] shows the droop-free operation of the device. The EQE is calculated using the formula [40] : $EQE = \frac{P \cdot e}{I \cdot h\upsilon}$, where e is the elementary charge, P is the optical power, I is the injected current, h is Planck's constant, and υ is the frequency of the emitted light. The EQE curve initially decreases, at very low injection currents, due to an overestimation of the EQE value, caused by the limitation of the silicon photodiode's working range (background noise level vs. received power). Afterwards, the EQE clearly rises at increased injection current due to the amplified optical power at the ASE regime, showing droop-free operation.

For further characterization of the SLD, Fig. 1(c) shows the emission spectra of the SLD when increasing the injection current, as measured with an optical spectrum analyzer (OSA, Yokowaga,

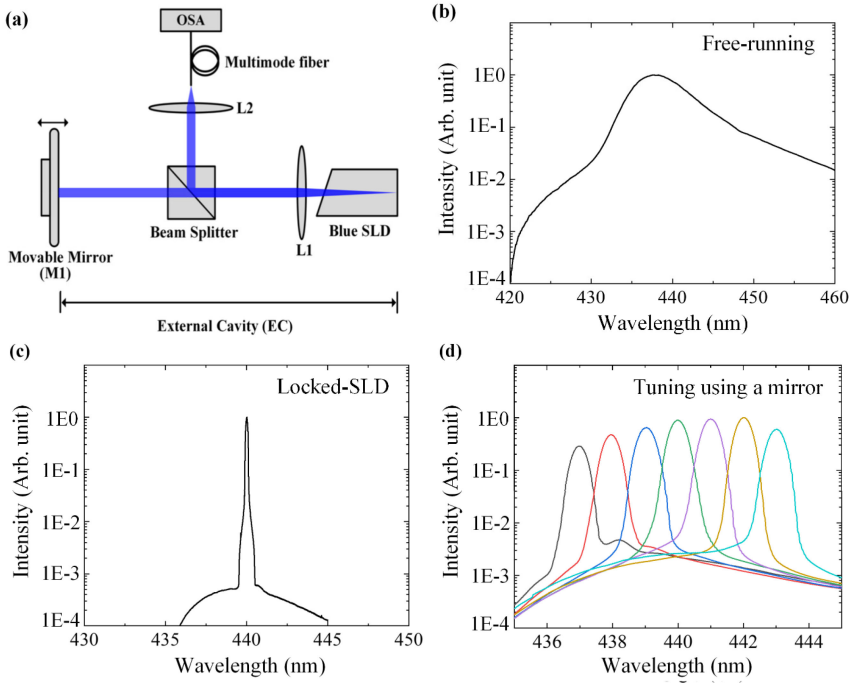

Fig. 2. (a) Experimental setup of the tunable single-wavelength laser designed using an SLD gain-chip and moving external mirror. Optical spectra of the free-running SLD (b), and the self-injection-locked SLD using a fixed EC (c) and using a tunable EC (d).

AQ6373B). The results of Fig. 1(c) are recorded when the SLD is biased using a pulsed injection current (1-kHz repetition rate, 15% duty-cycle) and at 20 °C using a benchtop laser current controller (Thorlabs, ITC4005) and a TEC mount (Thorlabs, TCLDM9), respectively. The peak emission wavelength shows a blue shift from 445 nm to 437 nm as shown in Fig. 1(d) [blue squares]. This blue-shift behavior can be attributed to the contributions of the screening of the quantum-confined Stark effect [41] and the band-filling effect [42], [43]. A peak red shift is observed in the emission spectra of the SLD operated from 700 mA to 1000 mA. This red shift from 437 nm to 438 nm is likely due to the increased non-radiative recombination at the gain saturation regime [39] together with the effect of a relatively large pulse duty cycle [44]. The SLD's optical bandwidth, measured as the full width at half maximum (FWHM) of the emission spectra [Fig. 1(d), blue circles], shows a reduction from ∼16.7 nm (50 mA) down to ∼5.1 nm (1000 mA). The FWHM in the ASE-dominated range of 200 mA to 800 mA decreases from ∼9 nm to 5.9 nm. These characteristics of the FWHM, together with the L–I curve and the EQE show a clear signature of SLD operation. In Fig. 1(d) [black dashed line] we have also plotted the slope efficiency (dP/dI) showing a peak value of up to 0.11 W/A. From the shape of the slope efficiency we notice a rate reduction at high injection currents. The flattening of the slope efficiency can be correlated to the gain saturation regime and peak emission red shift mentioned above, thus, suggesting the use of lower injection currents for optimal device operation. It is worth highlighting that the SLD has a far-field pattern with a lateral multimode emission similar to our previous report [37].

3. Single-Wavelength Laser Using an External Mirror

In this section, we demonstrate our first technique of combining the blue-light SLD with an EC configuration to design a single-wavelength laser. The experimental setup is shown schematically in Fig. 2(a) where the SLD's blue light is firstly collimated with an aspheric lens (L1, A110TM-A, Thorlabs) of a 6.24-mm focal length and a 0.4 numerical aperture (NA). The collimated light is

directed towards a beam splitter (BS) of a 92% (8%) transmissivity (reflectivity). The transmitted light through the BS is back-reflected via a movable mirror (M1) such that the SLD's (non-tilted) back facet and the M1 form an EC. As the laser beam is transmitted and reflected back through the same facet, it is termed a single-port device. The single-port gain medium eases the optical coupling requirements of the full system. The other reflected beam by the BS is forwarded in a direction of a collimating lens (L2) of a 35-mm focal length, which injects the blue light into a multimode fiber (MMF) of a 350-μm core diameter. The output end of the MMF is connected to the OSA to characterize the optical spectrum of the SLD's light. During this experiment, the SLD is driven by a pulsed injection current (385 mA, 1-kHz repetition rate, 15% duty-cycle) at 20 °C. Driving the SLD with a relatively high injection current may damage the device. Hence, we arbitrarily selected the 385-mA injection current for safe SLD operation, which can also induce stimulated emission using the SLD gain chip. The selected 385-mA current, which corresponds to a current density of 2.566 kA/cm^2, is not that high for GaN-based devices. As in [45], the threshold current of a high-power GaN blue laser is 300 mA. Additionally, characterizing the SLD-based laser at various injection currents is out of the scope of this work; however, it would generally follow the results of Figs. 1(b)-1(d).

Figure 2(b) shows the spectral profile of the free-running blue SLD; without including the M1 in the experimental setup. As expected, this profile exhibits a broad spectrum centered at a $\sim$438-nm wavelength with a 6.7-nm FWHM. In Fig. 2(c), we show a representative example when the SLD is self-injection locked using the external mirror M1 to generate a single spectral mode, with a linewidth limited by the resolution of the characterization method. A spectral-oriented characterization based on beating signals can be used to reveal the exact linewidth of this laser system [46]. Nevertheless, it is obvious that the broad optical spectrum of the free-running SLD is diminished because the SLD lases at a resolution-limited single mode. Thus, when adding the M1 into the system, one can reconfigure the SLD's operation to work in the lasing mode instead of the ASE regime, and thus reducing the FWHM. The switching time from lasing to ASE regime depends on the speed of alternating between engaging and disengaging an optical feedback via M1. By using a micro-electro-mechanical system (MEMS) based mirror, the M1 switching speed would be in the microsecond range [47]. Based on Ref. [48], the criteria for recognizing laser operation are (1) the narrow linewidth emission, (2) clear threshold in both output power and linewidth, (3) the light emission is characteristic of, and influenced by, the gain medium and the resonator, and (4) the light output consists of a beam. All of the first three conditions are demonstrated and satisfied in Figs. 1 and 2, together with a later discussion in optical power in Section 6. The condition (4) is naturally proven given the edge-emitting property of the SLD.

Since there is no internal cavity within the SLD, the free spectral range (FSR), $\Delta\lambda_{\text{FSR}}$, between two consecutive lasing wavelengths is only governed by the length (L_{ext}) of the EC as follows [40]:

$$\Delta\lambda_{\text{FSR}} \approx \frac{\lambda_c^2}{2nL_{\text{ext}}}, \tag{1}$$

where λ_c is the center wavelength of the SLD's blue light and n is the refractive index of the EC medium. In this experiment, $\lambda_c \sim 438$ nm, $L_{\text{ext}} \sim 25$ cm, and $n \sim 1$ which result in having a $\sim$0.38-pm mode spacing, using (1). By changing the external cavity's length, a 7-nm tuning spectral range starting from 436 nm to 443 nm is observed [Fig. 2(d)], with a resolution-limited FWHM of $\sim$0.5 nm. However, given the pm-scale of the mode spacing, the tuning is not possible to occur by only changing the length of the external cavity. Adjusting the cavity length within a range of half a wavelength results in a tuning range of approximately one free spectral range and in order to achieve wider tunability a dispersive element should be incorporated into the setup. The collimating lens we use in this setup exhibits chromatic aberration, causing a change in the focal length with the wavelength; thus, the lens can be considered as a dispersive element. The focal shift of the lens was estimated to be in the order of $\sim$7 μm, which is large compared to the Rayleigh length that is in the order of $\sim$3 μm. We conclude that the 7-nm tunability is then due to the chromatic focal shift of the collimating lens in combination with the movable mirror M1. The tilted facet, and thus the angled beam path, may also contribute to this chromatic shift. In other words, as M1 is moving,

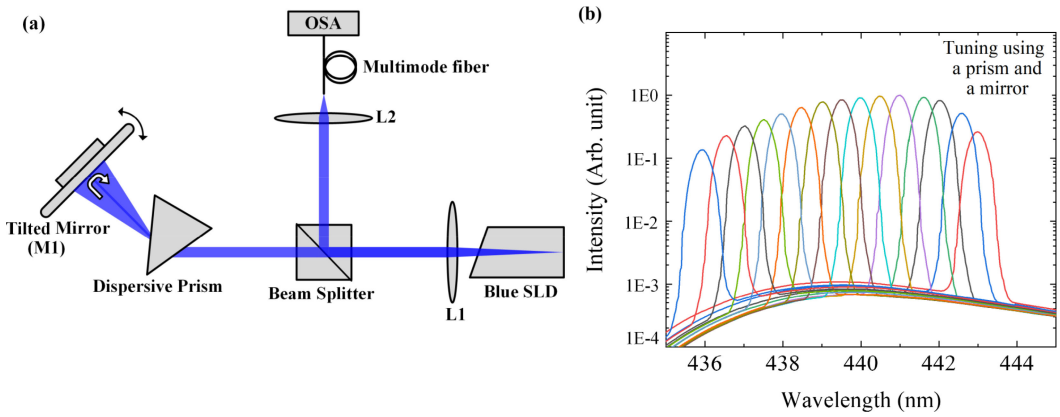

Fig. 3. (a) Experimental setup of a tunable single-wavelength laser using an SLD gain-chip, a mirror and a prism. (b) Optical spectra of the SLD as we tilt the mirror M1.

and considering the tilted facet contributing to non-perfect alignment, only a particular wavelength as determined by the chromatic focal shift of the collimating lens is focused back into the SLD to result in spectral tunability. The pm-scale FSR is relatively small; therefore, the spectral tuning can be considered continuous, as long as the dispersive element and the collimating lens feedback the desired wavelength. From the results in Fig. 2(d), we observe a ∼5-dB difference between the least and the most intense lasing modes. This is expected from the nonuniform gain profile of semiconductor devices [49]. It is worth mentioning that for the results in Figs. 2(c) and 2(d), the OSA resolution was set at 0.02 nm and 0.5 nm, respectively. Therefore, the FWHM of the lasing modes in these two figures cannot be compared directly.

Besides, it is worth mentioning that the wavelength tuning range is linked to the material system used to fabricate the laser and the range of wavelengths. For GaN-based lasers, a tuning of up to ∼6 nm is reported in the literature [50]. We report here a wavelength tuning from 436 nm (2.844 eV) to 443 nm (2.799 eV), i.e., a tuning range of ∼7 nm (44.67 meV). In contrast, a 1550 nm laser based on InP would have to be tunable over a ∼90-nm range, given the same energy tuning range.

4. Tunable Single-Wavelength Laser Using a Prism and an External Mirror

Here, we modify the experimental setup shown in Fig. 2(a) to include a dispersing equilateral prism placed in between the BS and M1 [Fig. 3(a)]. The main purpose of using the prism is to spatially resolve the spectral components of the SLD's blue light transmitted through the BS. Mirror M1 here is fixed onto a kinematic mount with fine adjustment screws. By tilting M1, as shown in Fig. 3(a), we can tune the wavelength of the light reflected back towards the SLD. The SLD's back facet and the M1 again create the EC such that the SLD is self-injection locked to lase at the spectral mode reflected by M1.

Figure 3(b) shows the spectral intensity profiles of the SLD as we tilt the mirror M1 using a kinematic mount. We can smoothly sweep the lasing modes over a ∼7-nm range, which is limited by the SLD's free-running spectral profile. An intensity equalization of up to ∼8.6 dB would be necessary for normalization of the laser modes. Since the SLD is always locked at the wavelength provided by the mirror, this experimental setup significantly mitigates the spectral mode-hopping. The FWHM values in Fig. 3(b) are also limited by the OSA's resolution limit (0.5 nm). Consequently, the impact of the prism on the FWHM was not investigated. By tilting the mirror M1, we can sweep along the wavelengths of the available self-injection-locked modes [Fig. 3(b)]. This is a major advantage for the EC-SLD design over its corresponding EC-laser diode counterparts. In typical EC-laser diode systems, the lengths of the external and internal cavities have to simultaneously satisfy the Fabry-Perot's constructive interference condition in order to lock a spectral mode,

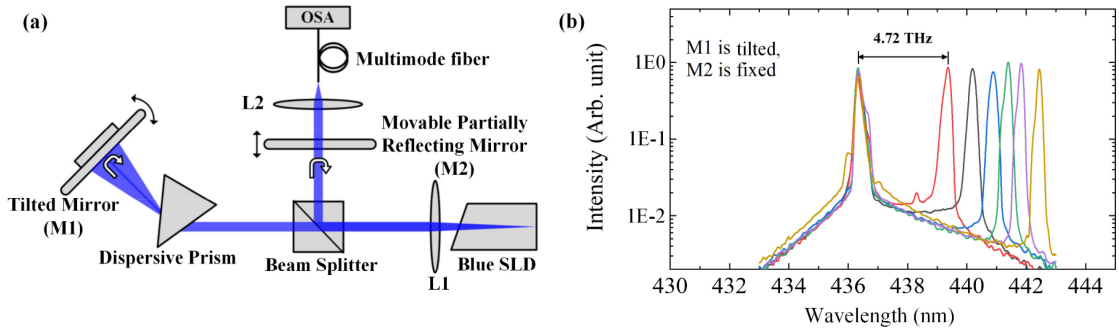

Fig. 4. (a) Experimental setup of the tunable dual-wavelength laser based on SLD gain-chip and external cavities. EC1 and EC2, which are established by incorporating M1 and M2, respectively. (b) Optical spectra of the SLD when M1 is tilted and M2 is fixed.

including those operating with various locking stages [51]. As a result, EC-laser diode systems typically require complicated and expensive setups to precisely control L_{ext}. Additionally, compared with the EC-SLD designs, the $\Delta\lambda_{FSR}$ of the EC-laser diodes is relatively coarse (in the nanometer range) because the internal cavity's length of a laser diode is typically hundreds of micrometers long [52].

In terms of the cost-effectiveness and simplicity, EC-laser diode such as the Littman Metcalf configuration [53] is comparable to our system. However, our SLD-based tunable laser configuration is more stable and mode-hopping-free, due to the properties described beforehand.

5. Tunable Dual-Wavelength SLD-Based Laser

We further modify our experimental setup to design a tunable dual-wavelength SLD-based laser which would find many important applications including terahertz (THz) wave generation by photomixing, sensing, biomedical imaging, among others [36], [54], [55]. In this design, one output wavelength is kept fixed while the other can be tuned across the entire spectral profile of the free-running SLD. The modified experimental setup is shown schematically in Fig. 4(a) where the collimated light from the SLD is directed towards a BS of 50:50 split ratio. The transmitted light through the BS is spectrally resolved with the dispersing equilateral prism, while the tilted mirror M1 forms the first EC (EC1) with the SLD's back facet. On the other hand, the reflected light from the BS is guided towards a partially reflecting mirror M2 of a 70% reflectivity, which is mounted onto a linear translational stage. This M2 mirror creates a second independent EC (EC2) with the back facet of the SLD. The transmitted light through the M2 is injected using the lens (L2) into the MMF to be spectrally analyzed on the OSA with a resolution of 0.1 nm. As mentioned above, creating an EC using the combined prism and mirror offers a more stable SLD-based tunable laser, compared with the case when only using the external mirror. This is because the prism resolves the spectral components of the SLD's blue light and consequently the SLD is easily locked at the wavelength reflected by M1. In contrast, relying only on the dispersive collimating lens along the path of M2 requires strict mechanical stability and perfect alignment to feedback a fixed wavelength into the SLD. However, for EC2, we use only the M2 without a prism. This is because the transmitted SLD's light through the M2 can be straightforwardly injected into the MMF, using L2, to be characterized on the OSA. In contrast, in case of adding a prism within the EC2, it is experimentally difficult to couple the SLD's spatially resolved light into the MMF. In other words, the purpose of using only the M2 in EC2 is just to prove the concept of the ability to design a tunable dual-wavelength SLD-based laser.

We fix M2 at an arbitrary position and keep tilting the other mirror, M1. As shown in Fig. 4(b), the SLD is self-injection locked to two spectral modes; a fixed mode of the EC2 [at 436.35 nm] and another tunable one of the EC1. In Fig. 4(b), we further show a representative example for a

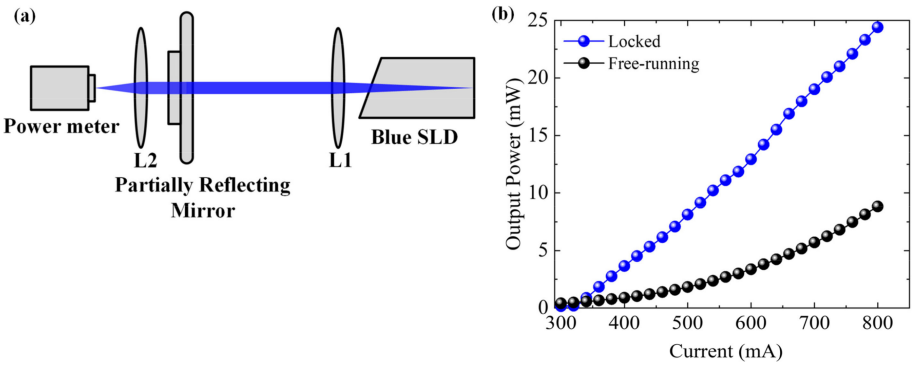

Fig. 5. (a) Experimental setup for measuring the SLD's optical power during the free-running and self-injection-locked operation. (b) Optical output power versus injected current (L-I) characteristics of both free-running and locked SLD operations.

possible spectral separation of 4.72 THz between the fixed and a tunable mode. Additionally, the spectral intensity equalization between two tunable modes is up to ∼1.3 dB, which can be easily corrected, for example, by utilizing variable neutral density filters. To the best of our knowledge, this is the first reported tunable dual-wavelength SLD-based laser in the visible range.

This SLD-based double EC configuration can be utilized as a laser source with a tunable THz frequency difference, which can be used as a light source in THz devices [36], [56]. The THz spectral difference of the dual-wavelength can be further extended via using a free-running SLD with a broader FWHM [57]. A future work should investigate the THz generation using the reported configuration. Additionally, owing to the droop-free operation and low speckle noise of the reported free-running SLD, our system could offer a large modulation bandwidth for visible-light communications (VLC) which has been demonstrated to make use of tunable lasers [58]. The tunable single/dual wavelength SLD-based laser is a potential transmitter for wavelength-division multiplexing (WDM) VLC systems. Incorporating the tunable SLD-based laser in a VLC system is contingent on generating a stable optical spectrum with minimal wavelength and FWHM fluctuations, which can significantly improve the performance of the VLC system [58].

It is also worth mentioning that tuning the emission wavelength of the SLD with external cavities outperforms the corresponding temperature-based tuning in two aspects. Firstly, the sensitivity of tuning GaN-lasers with temperature is well known to be relatively low, such as that of 0.06 nm/K reported in [59]. Thus, it would take a temperature change of 100 K to tune the emission over a 6-nm range. This can compromise the lifetime of the gain chip. Secondly, the temperature-based tuning cannot offer self-injection locking to the SLD.

6. Power Amplification Using the Self-Injection-Locked SLD

We further compare the optical power emitted by the SLD during the free-running and self-injection locked states at different injection current values. The experimental setup is shown schematically in Fig. 5(a) where the collimated light from the SLD is directed towards a partially reflecting mirror of 70% reflectivity. This mirror and the flat back facet of the SLD together form the EC. The transmitted light through the partially reflecting mirror is focused using the lens L2 onto an optical power meter. When the SLD is locked, it lases at ∼440-nm wavelength, with an average optical power of 3 mW with an injection current of 385 mA.

Transitioning from the self-injection locked state to the free-running state is achieved via tilting the partially reflecting mirror by a few degrees, which is sufficient to construct or destroy the EC. In the free-running case, the 70% partially reflecting mirror simply cuts 70% of the optical power delivered to the power meter. In a typical case of free-running SLD mode, this mirror would not be utilized. Therefore, we compensate for the losses the mirror introduces in the free-running case

via dividing the SLD's measured optical power by 0.3. At different injection currents, we show the estimated output power of the free-running SLD [Fig. 5(b), black circles]. Also, we plotted the directly measured power of the self-injection-locked SLD without compensation since the mirror is a part of the laser system [Fig. 5(b), blue circles]. At injection currents higher than ∼320 mA, where the locked SLD can achieve stimulated emission, we observe a significant amplification of the locked SLD's optical power, compared with the free-running case. For instance, at 500-mA injection current, the measured optical power of the self-injection-locked SLD is ∼4.46-fold (∼6.5 dB) the estimated output power of the free-running SLD. This observed optical amplification is a promising step towards designing a chip-based optical amplifier for the visible light. In comparison to traditional laser diodes, the lasing threshold current of a SLD system is relatively high [18]. In particular, the lasing threshold current of our reported EC-SLD equals ∼320 mA, whereas the threshold current of an equivalent GaN laser diode is ∼130 mA, as per our measurement (not shown here).

It is important to mention that the nearly-perfect linear L–I characteristic of the self-injection locked SLD indicates that the Fabry-Perot resonance cavity within the SLD is successfully suppressed. Otherwise, the L–I characteristic would be wavy due to the non-linearities and interferences between inner Fabry-Perot modes and the EC.

7. Discussion and Conclusion

In summary, we designed a single- and dual-wavelength tunable blue laser source using a single-port InGaN SLD under different EC configurations. The single-port characteristic eases optical coupling requirements on the system. Adding or removing the mirrors of the EC-SLD can reconfigure the device operation to work in the stimulated emission or the ASE regimes, giving an unparalleled capability to a single SLD gain chip. For the dual-wavelength operation, each spectral mode can be tuned independently, a feature of great interest for wave-mixing applications and reconfigurable laser photonics. The spectral tuning range of the reported laser sources extends from 436 nm to 443 nm which is limited by the optical gain profile of the free-running SLD, with wider tuning ranges expected from engineered InGaN gain media. Additionally, the SLD can offer light amplification up to ∼6.5 dB to the optical signal within the EC. Hence, our results provide a pathway for the development of next-generation single-chip reconfigurable platforms suitable for a wide range of applications, including biomedical applications, optical communication, and high-resolution spectroscopy.

Disclosures

The authors declare no conflicts of interest.

References

[1] A. Brodutch, R. Marchildon, and A. S. Helmy, "Dynamically reconfigurable sources for arbitrary gaussian states in integrated photonics circuits," *Opt. Exp.*, vol. 26, no. 13, Jun. 2018, Art. no. 17635.
[2] C. García-Meca *et al.*, "On-chip wireless silicon photonics: From reconfigurable interconnects to lab-on-chip devices," *Light Sci. Appl.*, vol. 6, Sep. 2017, Paper e17053.
[3] Y. Ozeki, T. Asai, J. Shou, and H. Yoshimi, "Multicolor stimulated raman scattering microscopy with fast wavelength-tunable yb fiber laser," *IEEE J. Sel. Topics Quantum Electron.*, vol. 25, no. 1, Jan. 2019, Art. no. 7100211.
[4] E. Bruce, "Tunable lasers," *IEEE Spectr.*, vol. 39, no. 2, pp. 35–39, 2002.
[5] S. Yin *et al.*, "Wavelength multiplexed holographic storage in a sensitive photorefractive crystal using a visible-light tunable diode laser," *Opt. Commun.*, vol. 101, no. 5, 6, pp. 317–321, Sep. 1993.
[6] L. K. Cheng, W. R. Bosenberg, and C. L. Tang, "Broadly tunable optical parametric oscillation in β-BaB_2O_4," *Appl. Phys. Lett.*, vol. 53, no. 3, pp. 175–177, Jul. 1988.
[7] N. Granzow, "Supercontinuum white light lasers: A review on technology and applications," in *Proc. SPIE*, 2019, Art. no. 1114408.
[8] B. Mroziewicz, "External cavity wavelength tunable semiconductor lasers-a review," *Opto-Electron. Rev.*, vol. 16, no. 4, pp. 347–366, Jan. 2008.

[9] M. Chi, O. Bjarlin Jensen, A. Kragh Hansen, and P. Michael Petersen, "Tunable high-power external-cavity GaN diode laser systems in the visible spectral range," in *Proc. Laser Technol. Its Appl., IntechOpen*, 2019, pp. 3–22.
[10] J. Buus and E. J. Murphy, "Tunable lasers in optical networks," *J. Light. Technol.*, vol. 24, no. 1, pp. 5–11, Jan. 2006.
[11] H. Okamoto, K. Kasuga, I. Hara, and Y. Kubota, "Ultra-wideband tunable RGB fiber laser," in *Proc. Conf. Lasers Electro-Opt./Int. Quantum Electron. Conf.*, 2009, Art. no. CFB7.
[12] M. Chi, O. B. Jensen, A. K. Hansen, and P. M. Petersen, "Dynamics of a green high-power tunable external-cavity broad-area GaN diode laser," *JOSA*, vol. 35, no. 4, pp. 667–671, Apr. 2018.
[13] D. J. Lonsdale, A. P. Willis, and T. A. King, "Extended tuning and single-mode operation of anti-reflection-coated InGaN violet laser diode in a Littrow cavity," *Meas. Sci. Technol.*, vol. 13, pp. 488–493, 2002.
[14] L. Hildebrandt, R. Knispel, S. Stry, J. R. Sacher, and F. Schael, "Antireflection-coated blue GaN laser diodes in an external cavity and Doppler-free indium absorption spectroscopy," *Appl. Opt.*, vol. 42, no. 12, pp. 2110–2118, 2003.
[15] H. Ohno, K. Orita, M. Kawaguchi, K. Yamanaka, and S. Takigawa, "200 mW GaN-based superluminescent diode with a novel waveguide structure," in *Proc. IEEE Photonic Soc. 24th Annu. Meet.*, 2011, pp. 505–506.
[16] A. Kafar, S. Stanczyk, D. Schiavon, T. Suski, and P. Perlin, "Rev.—Rev. Optim. Curr. Status (Al,In)GaN superluminescent diodes," *ECS Journal Solid State Science Technology*, vol. 9, no. 1, Nov. 2020, Art. no. 015010.
[17] C.-F. Lin, M.-J. Chen, and B.-L. Lee, "Wide-range tunable dual-wavelength semiconductor laser using asymmetric dual quantum wells," *IEEE Photon. Technol. Lett.*, vol. 10, no. 9, pp. 1208–1210, Sep. 1998.
[18] F.-W. Sheu and P.-L. Luo, "Development of a variable spectral-width, wavelength-tunable light source using a superluminescent diode with optical feedback," *Amer. J. Phys.*, vol. 76, no. 8, pp. 769–776, Aug. 2008.
[19] S. H. Oh *et al.*, "L-band tunable external cavity laser based on 1.58 μm superluminescent diode integrated with spot-size converter," *Opt. Exp.*, vol. 18, no. S3, pp. A300–A306, 2010.
[20] Y. Zheng, T. Kurita, T. Sekine, Y. Kato, and T. Kawashima, "Tunable continuous-wave dual-wavelength laser by external-cavity superluminescent diode with a volume bragg grating and a diffraction grating," *Appl. Phys. Lett.*, vol. 109, 2016, Art. no. 141107.
[21] E. V. Andreeva *et al.*, "Tunable laser based on a semiconductor optical amplifier of red spectral region," *Quantum Electron.*, vol. 49, no. 5, pp. 493–496, May 2019.
[22] T. Weig, H. Höck, K. Holc, K. Köhler, J. Wagner, and U. T. Schwarz, "Implementation and investigation of mode locking in GaN-based laser diodes in external cavity configuration," *Phys. Status Solidi Appl. Mater. Sci.*, vol. 212, no. 5, pp. 986–991, 2015.
[23] S. Gee and J. E. Bowers, "Ultraviolet picosecond optical pulse generation from a mode-locked InGaN laser diode," *Appl. Phys. Lett.*, vol. 79, no. 13, pp. 1951–1952, Sep. 2001.
[24] C. Shen *et al.*, "Group-III-Nitride superluminescent diodes for solid-state lighting and high-speed visible light communications," *IEEE J. Sel. Topics Quantum Electron.*, vol. 25, no. 6, Nov. 2019, Art. no. 2000110.
[25] N. Primerov *et al.*, "A compact red-green-blue superluminescent diode module: A novel light source for AR microdisplays," in *Proc. SPIE*, 2019, Art. no. 110620F.
[26] G. R. Goldberg *et al.*, "Gallium nitride superluminescent light emitting diodes for optical coherence tomography applications," *IEEE J. Sel. Topics Quantum Electron.*, vol. 23, no. 6, Nov. 2017, Art. no. 2000511.
[27] E. Feltin *et al.*, "Broadband blue superluminescent light-emitting diodes based on GaN," *Appl. Phys. Lett.*, vol. 95, no. 8, 2009, Art. no. 081107.
[28] F. Kopp *et al.*, "Blue superluminescent light-emitting diodes with output power above 100 mW for picoprojection," *Jpn. J. Appl. Phys.*, vol. 52, no. 8S, 2013, Art. no. 08JH07.
[29] C. Shen *et al.*, "High-brightness semipolar (2021) blue InGaN/GaN superluminescent diodes for droop-free solid-state lighting and visible-light communications," *Opt. Lett.*, vol. 41, no. 11, pp. 2608–2611, 2016.
[30] R. Cahill, P. P. Maaskant, M. Akhter, and B. Corbett, "High power surface emitting InGaN superluminescent light-emitting diodes," *Appl. Phys. Lett.*, vol. 115, no. 17, Oct. 2019, Art. no. 171102.
[31] K. Vizbaras *et al.*, "High power continuous-wave GaSb-based superluminescent diodes as gain chips for widely tunable laser spectroscopy in the 1.95–2.45 μm wavelength range," *Appl. Phys. Lett.*, vol. 107, Jul. 2015, Art. no. 011103.
[32] F. J. Hu, P. Jin, Y. H. Wu, F. F. Wang, H. Wei, and Z. G. Wang, "Broadband and high-speed swept external-cavity laser using a quantum-dot superluminescent diode as gain device," *Chin. Phys. B*, vol. 24, no. 10, 2015, Art. no. 104212.
[33] A. Takamizawa, S. Yanagimachi, and T. Ikegami, "Generation of incoherent light from a laser diode subject to external optical injection from a superluminescent diode," *Appl. Opt.*, vol. 53, no. 3, pp. 435–440, 2014.
[34] H. M. Oubei *et al.*, "Light based underwater wireless communications," *Jpn. J. Appl. Phys.*, vol. 57, no. 8S2, 2018, Art. no. 08PA06.
[35] M. Ohmi, M. Tanizawa, A. Fukunaga, and M. Haruna, "In-situ observation of tissue laser ablation using optical coherence tomography," *Opt. Quantum Electron.*, vol. 37, pp. 1175–1183, Dec. 2005.
[36] P. Gu, F. Chang, M. Tani, K. Sakai, and C.-L. Pan, "Generation of coherent cw-Terahertz radiation using a tunable dual-wavelength external cavity laser diode," *Jpn. J. Appl. Phys.*, vol. 38, no. Part 2, pp. L1246–L1248, Nov. 1999.
[37] A. A. Alatawi *et al.*, "High-power blue superluminescent diode for high CRI lighting and high-speed visible light communication," *Opt. Exp.*, vol. 26, no. 20, Oct. 2018, Art. no. 26355.
[38] K. Holc *et al.*, "Temperature dependence of superluminescence in ingan-based superluminescent light emitting diode structures," *J. Appl. Phys.*, vol. 108, no. 1, 2010, Art. no. 013110.
[39] S. Stanczyk *et al.*, "450 nm (Al,In)GaN optical amplifier with double 'j-shape' waveguide for master oscillator power amplifier systems," *Opt. Exp.*, vol. 26, no. 6, Mar. 2018, Art. no. 7351.
[40] L. A. Coldren, S. W. Corzine, and M. L. Mašanović, *Diode Lasers and Photonic Integrated Circuits*, 2nd ed. Hoboken, NJ, USA: Wiley, 2012.
[41] A. Kafar, S. Stanczyk, S. Grzanka, K. Pieniak, T. Suski, and P. Perlin, "Screening of quantum-confined stark effect in nitride laser diodes and superluminescent diodes," *Appl. Phys. Exp.*, vol. 12, no. 4, Apr. 2019, Art. no. 044001.
[42] H. C. Casey, J. Muth, S. Krishnankutty, and J. M. Zavada, "Dominance of tunneling current and band filling in InGaN/AlGaN double heterostructure blue light-emitting diodes," *Appl. Phys. Lett.*, vol. 68, no. 20, pp. 2867–2869, May 1996.

[43] H. C. Casey and R. Z. Bachrach, "Electroluminescent shifting-peak spectra in GaAs with uniform excitation," *J. Appl. Phys.*, vol. 44, no. 6, pp. 2795–2804, Jun. 1973.
[44] S. Figge, T. Böttcher, D. Hommel, C. Zellweger, and M. Ilegems, "Heat generation and dissipation in GaN-based light emitting devices," *Phys. Status Solidi*, vol. 200, no. 1, pp. 83–86, Nov. 2003.
[45] Y. Nakatsu *et al.*, "Blue and green InGaN semiconductor lasers as light sources for displays," in *Proc. SPIE*, 2020, Art. no. 112800S.
[46] B. C. Young, F. C. Cruz, W. M. Itano, and J. C. Bergquist, "Visible lasers with subhertz linewidths," *Phys. Rev. Lett.*, vol. 82, no. 19, pp. 3799–3802, 1999.
[47] W. M. Mellette and J. E. Ford, "Scaling limits of MEMS beam-steering switches for data center networks," *J. Light. Technol.*, vol. 33, no. 15, pp. 3308–3318, Aug. 2015.
[48] I. D. W. Samuel, E. B. Namdas, and G. A. Turnbull, "How to recognize lasing," *Nat. Photon.*, vol. 3, pp. 546–549, 2009.
[49] T. Lermer *et al.*, "Gain of blue and cyan InGaN laser diodes," *Appl. Phys. Lett.*, vol. 98, 2011, Art. no. 021115.
[50] M. Chi, O. B. Jensen, and P. M. Petersen, "Tuning range and output power optimization of an external-cavity GaN diode laser at 455 nm," *Appl. Opt.*, vol. 55, no. 9, 2016, Art. no. 2263.
[51] M. H. M. Shamim, T. K. Ng, B. S. Ooi, and M. Z. M. Khan, "Single and multiple longitudinal wavelength generation in green diode lasers," *IEEE J. Sel. Topics Quantum Electron.*, vol. 25, no. 6, 2019, Art. no. 1501307.
[52] H. Zhang *et al.*, "Short cavity ingan-based laser diodes with cavity length below 300 μm," *Semicond. Sci. Technol.*, vol. 34, no. 8, Aug. 2019, Art. no. 085005.
[53] W. Wang, A. Major, and J. Paliwal, "Grating-stabilized external cavity diode lasers for Raman spectroscopy—A review," *Appl. Spectrosc. Rev.*, vol. 47, no. 2, pp. 116–143, Feb. 2012.
[54] D. Liu, N. Q. Ngo, S. C. Tjin, and X. Dong, "A dual-wavelength fiber laser sensor system for measurement of temperature and strain," *IEEE Photon. Technol. Lett.*, vol. 19, no. 15, pp. 1148–1150, Aug. 2007.
[55] P. Bakopoulos, I. Karanasiou, N. Pleros, P. Zakynthinos, N. Uzunoglu, and H. Avramopoulos, "A tunable continuous wave (CW) and short-pulse optical source for THz brain imaging applications," *Meas. Sci. Technol.*, vol. 20, no. 10, Oct. 2009, Art. no. 104001.
[56] Y. Zheng, T. Sekine, T. Kurita, Y. Kato, and T. Kawashima, "Continuous-wave dual-wavelength operation of a distributed feedback laser diode with an external cavity using a volume Bragg grating," *Jpn. J. Appl. Phys.*, vol. 57, no. 3, 2018, Art. no. 030307.
[57] A. Kafar *et al.*, "InAlGaN superluminescent diodes fabricated on patterned substrates: An alternative semiconductor broadband emitter," *Photon. Res.*, vol. 5, no. 2, pp. A30–A34, 2017.
[58] S. Mukhtar, S. Xiaobin, I. Ashry, T. K. Ng, B. S. Ooi, and M. Z. M. Khan, "Tunable violet laser diode system for optical wireless communication," *IEEE Photon. Technol. Lett.*, vol. 32, no. 9, pp. 546–549, May 2020.
[59] S. Nakamura *et al.*, "Violet ingan/gan/algan-based laser diodes with an output power of 420 mW," *Jpn. J. Appl. Phys.*, vol. 37, no. Part 2, 6A, pp. L627–L629, 1998.